

# Contact Mechanics of Nanometer-Scale Molecular Contacts: Correlation between Adhesion, Friction, and Hydrogen Bond Thermodynamics

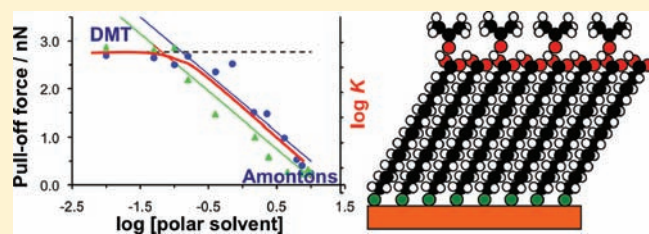
Katerina Busuttill,<sup>†</sup> Mark Geoghegan,<sup>‡</sup> Christopher A. Hunter,<sup>†</sup> and Graham J. Leggett<sup>\*,†</sup>

<sup>†</sup>Department of Chemistry, University of Sheffield, Brook Hill, Sheffield S3 7HF, U.K.

<sup>‡</sup>Department of Physics and Astronomy, University of Sheffield, Sheffield S3 7RH, U.K.

**ABSTRACT:** Using a scanning force microscope, adhesion forces have been measured between carboxylic acid terminated self-assembled monolayers in different nonpolar solvents or in two-component liquid mixtures consisting of a polar solvent (ethyl acetate or acetone) in heptane. The adhesion forces measured in pure acetone and ethyl acetate were small (0.24 nN) but increased logarithmically as the concentration of the polar solvent decreased to reach a maximum value (2.77 nN), equal to that measured in pure heptane, and for lower concentrations of polar solvent, the adhesion force remained constant.

This behavior is identical to that observed for association constants measured for the formation of 1:1 H-bonded complexes between dilute solutes in solvent mixtures. The transition between the solvent-dependent and -independent regimes occurs at a polar solvent concentration corresponding to  $1/K_S$ , where  $K_S$  is the equilibrium constant for solvation of a carboxylic acid by the polar solvent in heptane. A simple model, in which the solvation of the carboxylic acid groups may be estimated by considering the concentration and polarity of functional groups in the liquid, accurately predicts values of  $K_S$  that were found to correlate very well with the observed solvent-dependence of the adhesion force. Friction–load relationships were measured using friction–force microscopy. In pure acetone and ethyl acetate, a linear friction–load relationship was observed, in agreement with Amontons’ law. However, as the concentration of polar solvent was reduced, a nonlinear relationship was observed and the friction–load relationship was found to fit the Derjaguin–Müller–Toporov (DMT) model for single asperity contacts. For pure heptane and a range of other nonpolar liquids with identical dielectric constants, the friction–load relationship was described by DMT mechanics. Exceptionally, for perfluorodecalin, Johnson–Kendall–Roberts mechanics was observed. These observations may be rationalized by treating the friction force as the sum of load-dependent and shear contributions. Under conditions of low adhesion, where the carboxylic acid surface is solvated by polar solvent molecules, the shear term is negligible and the sliding interaction is dominated by load-dependent friction. As the degree of solvation of the carboxylic acid groups decreases and the adhesion force increases, the shear friction contribution increases, dominating the interaction for media in which the adhesion force is greater than ca. 0.6 nN.



## INTRODUCTION

Friction occurs in all moving mechanical contacts, and lubrication is consequently one of the oldest and most ubiquitous branches of engineering.<sup>1</sup> Molecular materials play a prominent role in the control of interfacial friction. Classically, amphiphilic molecules lubricate sliding contacts in mechanical devices. Recently, new technologies have created the need for an enhanced understanding of the behavior of molecules in nanometer-scale mechanical contacts.<sup>2</sup> For example, microelectromechanical systems (MEMS) contain miniaturized mechanical components that cannot be lubricated by conventional means; there is thus a need for new lubricants to control the frictional interactions. One potential solution is to use a self-assembled monolayer (SAM) of alkylsilanes.

In friction force microscopy (FFM), a variant of scanning force microscopy (SFM),<sup>3–5</sup> the lateral deflections of a cantilever are measured as the tip slides across the sample surface; as the strength of the frictional interaction between the tip and the

surface increases, so the lateral deflection of the cantilever increases. FFM is based upon the interaction between a single, well-defined asperity (the SFM probe) and the surface; it thus presents a model system with which to explore nanometer scale tribological phenomena. However, from a chemical perspective, it also offers many other possibilities. Friction forces measured by FFM are exquisitely sensitive to nanometer-scale molecular structure: energy dissipation in the sliding contact between the tip and sample is determined by the nature of any noncovalent interactions across the tip–sample interface,<sup>6–12</sup> the packing density,<sup>9,13,14</sup> and the organization of molecules. Hence FFM measurements facilitate the mapping of variations in surface chemical composition at nanometer resolution,<sup>15</sup> the measurement of the rates of surface chemical reactions in small regions,<sup>16,17</sup> and

Received: February 4, 2011

Published: May 11, 2011

the prospect of investigating many types of molecular interactions at interfaces. Here we demonstrate that careful analysis of pull-off forces made in liquid mixtures may yield fundamental data on the thermodynamics of noncovalent interactions in condensed phases.

Central to the development of FFM as a tool for the investigation of molecular interfaces is the acquisition of an adequately firm understanding of the mechanics of interaction between the tip and counterface. Such an understanding is currently lacking. While some authors have modeled the tip-sample interaction using single asperity contact mechanics models, such as the Johnson–Kendall–Roberts (JKR) model and the Derjaguin–Müller–Toporov (DMT) model, others have utilized Amontons' law. In the single asperity models, the friction force  $F_F$  varies approximately with  $F_N^{2/3}$ , where  $F_N$  is the load, while, in Amontons' law,  $F_F = \mu F_N$  where  $\mu$  is the coefficient of friction. The meaning of the "coefficient of friction" in an experiment involving contact between a single asperity and a planar surface remains opaque, given that Amontons' law is typically said to be explained by interactions between multiple microscopic asperities at two interacting macroscopic surfaces.

As long as the mechanics of interaction remain uncertain, the interpretation of FFM data will remain problematic. Recently, a number of papers have addressed this fundamental obstacle. Gao et al. made the radical suggestion that single asperity mechanics represent a limiting case where the strength of adhesion between tip and surface is very large.<sup>18</sup> They argued that a linear friction–load relationship is to be expected under most circumstances and that the friction force is determined not by the area of contact (as has usually been assumed previously<sup>1</sup>) but by the net interaction energy across the interface. Experimental studies of poly(ethylene terephthalate)<sup>19</sup> and self-assembled monolayer surfaces<sup>20</sup> yielded JKR mechanics in perfluorodecalin (where adhesion forces were large) and Amontons-type behavior in ethanol (where adhesion forces were much smaller). Other work suggests that not only the strength of adhesion but also the nature of the contact mechanics varies with the nature of the medium in which sliding occurs.<sup>21</sup> Based on modeling using molecular dynamics,<sup>22</sup> Mo et al. concluded that the friction force varied with the number of atomic contacts and, hence, that the friction–load relationship was linear.

The existing literature is, in general, notable for its failure to give adequate attention to the role played by the medium in which sliding occurs. Here we address this concern by measuring adhesion and friction forces in liquid mixtures for carboxylic acid terminated SAMs. Because the Hamaker constant is known to depend upon the dielectric constant  $\epsilon$  of the liquid medium, we chose two systems, heptane/acetone and heptane/ethyl acetate, for which there is a smooth relationship between  $\epsilon$  and composition. Our hypothesis was that the interaction force between tip and sample would increase as the value of  $\epsilon$  decreased. While adhesion forces were larger in media with smaller dielectric constants, we found that the dielectric constant is in fact a poor predictor of interaction strengths. Instead, using a simple model for hydrogen bonding based upon consideration of solvation of the carboxylic acid groups by polar functional groups in the solvent, we found a good correlation between the solvent-dependence of the surface pull-off forces and solution-phase equilibrium constants for the formation of 1:1 H-bonded complexes. The strength of adhesion and the type of contact mechanics may be rationalized, for surfaces containing carboxylic acid groups, in terms of the degree of solvation of the surface by polar molecules. In contrast to Gao et al.,<sup>18</sup> we find that the best way to explain these data is to

treat the friction force as the sum of load-dependent and adhesion-dependent terms, and we conclude that Amontons-type behavior represents, for hydrogen-bonding surfaces in polar liquids, a limiting case where the surface is extensively solvated.

## EXPERIMENTAL SECTION

**Au-Coated Substrates and Scanning Force Microscopy Probes.** Glass slides (Menzel-Gläser 22 mm × 64 mm, #1.5) and commercial V-shaped Si<sub>3</sub>N<sub>4</sub> scanning force microscopy probes (Veeco Instruments, Santa Barbara, CA) with a nominal spring constant of 0.06 N m<sup>-1</sup> were cleaned with piranha solution, H<sub>2</sub>SO<sub>4</sub>/H<sub>2</sub>O<sub>2</sub>, 70:30 (v/v) to remove all traces of organic material, including a polydimethylsiloxane contaminant.<sup>23</sup> (*Caution! Piranha solution is a strong oxidizing agent and should be handled with care.*) The slides and probes were rinsed with deionized water (18.2 MΩ cm) and dried in an oven at 150 °C.

The SFM probes were then coated with a 1 nm Cr layer at a rate of 0.03 nm s<sup>-1</sup> (Cr chips, 99.99% purity, Agar Scientific), followed by a 10 nm Au layer (Au wire, 99.99% purity, Advent Research Materials Ltd.) deposited at 0.03 nm s<sup>-1</sup> in an Edwards Auto 306 bell jar vacuum coater system. Glass slides were coated with a 10 nm Cr layer at a rate of 0.03 nm s<sup>-1</sup> followed by a 50 nm Au layer at 0.03 nm s<sup>-1</sup>.

**Preparation of Self-Assembled Monolayers.** 11-Mercaptoundecanoic acid (99% purity, Sigma-Aldrich) was used as received. Thiolate monolayers were prepared immediately after gold deposition by immersion of the freshly coated SFM probes and slides in 1 mM solutions of thiol in degassed ethanol for approximately 18 h at room temperature. Modified probes and slides were rinsed in copious amounts of degassed ethanol and dried in a stream of N<sub>2</sub> gas.

**Solvents Used in FFM Experiments.** *n*-Heptane (HPLC, Fisher Scientific), ethyl acetate (HPLC, Fisher Scientific), *n*-hexadecane (99%, Sigma-Aldrich), toluene (HPLC, Fisher Scientific), acetone (HPLC, Fisher Scientific), *cis,trans*-perfluorodecalin (95%, Sigma-Aldrich), ethanol (HPLC, Fisher Scientific), *n*-decane (≥99% Sigma Aldrich), and *n*-dodecane (≥99% Sigma Aldrich) were all used as received and injected into the SFM fluid cell using a disposable 1 mL syringe.

**Friction Force Microscopy.** Friction force measurements were acquired on a Multimode Nanoscope (IV) (Veeco Instruments, Santa Barbara, CA) scanning force microscope operating in contact mode with the fast scan direction perpendicular to the long axis of the cantilever, collecting both topographic and frictional data. The photodetector sensitivity was calibrated prior to each experiment by recording a plot of photodetector signal versus cantilever displacement when the probe was in contact with a very stiff sample, such as mica. Normal spring constants were obtained for each coated probe using a method that approximates a cantilever to a harmonic oscillator where cantilever motion is driven by thermal noise. The cantilever's response was correlated with the spring constant using a relationship derived by Hutter and Bechhoefer.<sup>24</sup>

Torsional spring constants were obtained at the end of each set of experiments using a calibration grid (TGF11, MikroMasch, CA) as described by Varenberg et al.<sup>25</sup> and Tocha et al.<sup>26</sup> Tip radii were calculated using a calibration grid (TGG01, MikroMasch, CA) and SPIP software.

The frictional force between two contacting surfaces is half the resultant force obtained for the forward and reverse signal recorded by the photodetector.<sup>27</sup> The photodetector response was plotted against the load for each system over a scan size of 3 μm × 3 μm employing a scan rate of 2.98 Hz. In each experiment, the load was reduced from ~20–35 nN in 0.2–0.1 V steps down to a point at which contact between the two surfaces was broken. In order to reduce systematic errors in the lateral force measurements, at the start of each experiment care was taken to ensure that the lateral deflection signal was zero when zero load was applied. Each set of experiments was repeated using

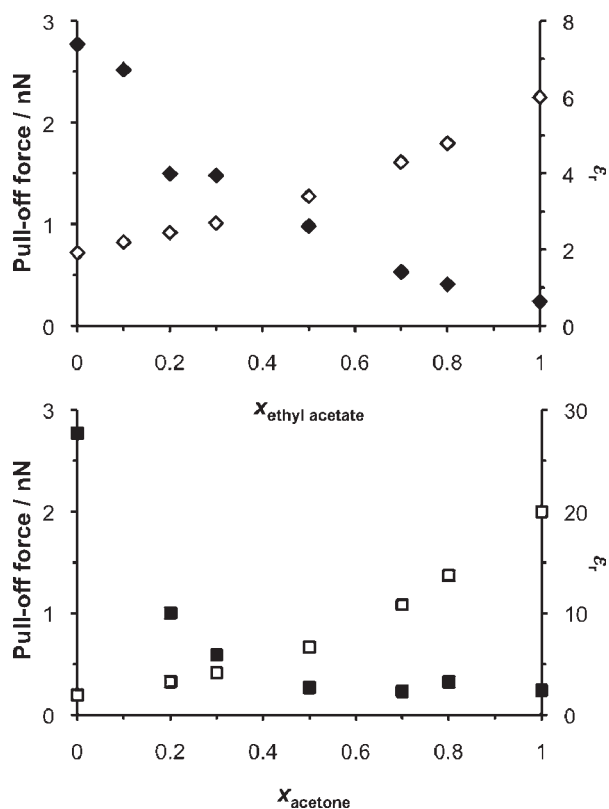


**Figure 1.** Relative dielectric constants  $\epsilon_r$  (open symbols) and pull-off forces (filled symbols), measured in ethyl acetate/heptane (top) and acetone/heptane (bottom) mixtures, as a function of the mole fraction of the polar solvent for mercaptoundecanoic acid SAMs deposited onto gold-coated glass substrates and gold-coated SFM probes. The error bars are smaller than the size of the symbols used to mark points.

different samples and different probes on different days to verify that data were reproducible. Data were collected at a minimum of five different locations on the sample surface for friction load plots, and force curves were obtained at a minimum of 500 locations on the sample surface for each solvent type. Pull-off forces were extracted from the data using Matlab software and Carpick's Toolbox.<sup>28</sup>

## RESULTS

**Measurement of Adhesion Forces.** Pull-off (adhesion) forces were measured for SAMs of mercaptoundecanoic acid SAMs deposited onto gold-coated glass substrates and gold-coated SFM probes in acetone/heptane and ethyl acetate/heptane liquid mixtures. Figure 1 shows data for both mixtures, together with the respective relative dielectric constants. It may be seen that the pull-off force increases as the mole fraction of the nonpolar solvent increases. In both pure ethyl acetate and pure acetone, the pull-off force is 0.24 nN, which rises, as the mole fraction of heptane increases, to a value over ten times greater than this. While the relative dielectric constants for pure acetone and ethyl acetate are quite different, no significant difference was observed in the pull-off forces measured in these liquids.

To examine the relationship between the pull-off force and the relative dielectric constant, both sets of data were combined and plotted in Figure 2. Additionally, to extend the range of comparison, data were acquired for interactions between carboxylic acid terminated SAMs in ethanol and in four nonpolar liquids (decane, dodecane, hexadecane, and perfluorodecalin). It may

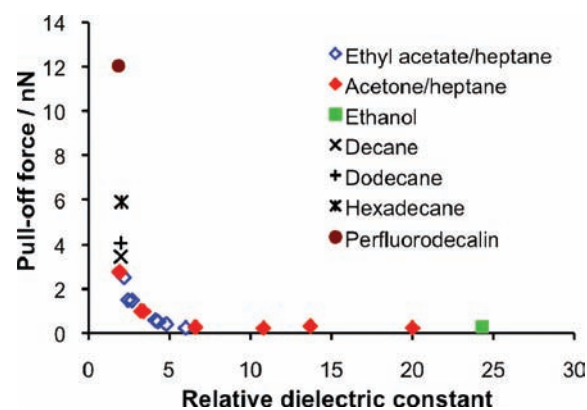


**Figure 2.** Variation in the pull-off force with the relative dielectric constant for liquid mixtures containing heptane and a more polar solvent (ethyl acetate, open blue diamonds, or acetone, filled red diamonds), together with data for pure ethanol and four nonpolar liquids. The error bars are smaller than the size of the symbols used to mark points.

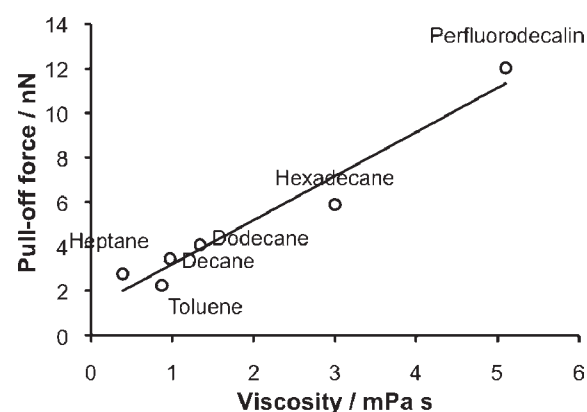


**Figure 3.** Variation in the pull-off force with viscosity for nonpolar liquids ( $1.86 < \epsilon_r < 2.04$ ). The error bars are comparable in size to the symbols used to mark points.

be seen from Figure 2 that, for liquids with  $\epsilon_r > 5$ , there was little change in the magnitude of the pull-off force as a function of the relative dielectric constant. Conversely, for the pure nonpolar liquids, a wide range of pull-off forces was observed for liquids with very similar values of  $\epsilon_r$ .

Figure 3 shows the pull-off forces for the nonpolar liquids as a function of their viscosity. It is clear that the pull-off force increases with viscosity and that the relationship is approximately linear. The explanation for this is not clear, but it is likely that the pull-off experiment is rate-dependent; as the viscosity of the fluid medium increases, then the rate of pulling decreases and the adhesion force increases. This emphasizes the difficulties associated with making comparative force microscopy measurements in different liquid media. However, (nonpolar) heptane and (polar) ethyl acetate have very similar viscosities (0.39 and 0.45 mPa s, respectively), and while the viscosity of (polar) acetone (0.79 mPa s) is only slightly greater than that of ethyl acetate, the similarity in the pull-off forces measured for the pure polar liquids (which were identical within experimental error) compared to those measured in heptane (which were more than an order of magnitude greater) suggests that changes in viscosity make a negligible contribution to the changes in pull-off force that were observed as a function of liquid composition in Figure 1.



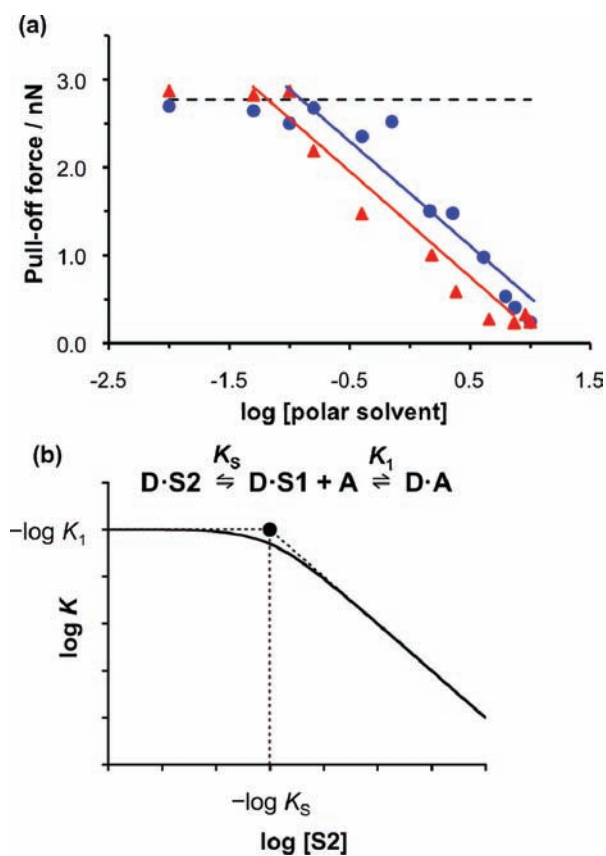


**Figure 4.** (a) Variation in the pull-off force with  $\log[\text{polar solvent}]$ , where  $[\text{polar solvent}]$  is the concentration of polar solvent. Red triangles: acetone/heptane. Blue circles: ethyl acetate/heptane. The horizontal line corresponds to the pull-off force in pure heptane. The error bars are smaller than the size of the symbols used to mark points. (b) Variation in  $\log K$  for formation of a 1:1 complex between two solutes (a H-bond acceptor, A, and a H-bond donor, D) in mixtures of a nonpolar solvent (S1) and a polar solvent (S2), which contains a good H-bond acceptor group and no good H-bond donors.  $K_1$  is the equilibrium constant for formation of the A•D complex in solvent S1, and  $K_S$  is the equilibrium constant for solvation of D by S2 in solvent S1.

In Figure 4a, the adhesion force is shown as a function of the concentration of the polar solvent. As  $[\text{polar solvent}]$  was decreased, the adhesion force increased, up to a limiting value corresponding to that measured in pure heptane. A horizontal line is shown corresponding to the pull-off force measured in pure heptane. At low concentrations of the polar solvent, the points may be seen to lie on this line. Straight lines can also be fit to the data in the region where the pull-off force increased with decreasing polar solvent concentration. The intercepts between these lines of best fit and the pure heptane line occurred at values of  $\log [\text{polar solvent}]$  of  $-1.2$  (corresponding to  $0.06 \text{ mol dm}^{-3}$ ) for acetone/heptane and  $-0.8$  ( $0.14 \text{ mol dm}^{-3}$ ) for ethyl acetate/heptane.

One of us has previously investigated hydrogen bonding in solvent mixtures and shown that solvation in liquid mixtures can be understood at the molecular level by considering the polarities and the concentrations of the functional groups present. The association constant,  $K$ , for formation of a 1:1 complex between a hydrogen bond donor, D, and a hydrogen bond acceptor, A, in a mixture of a nonpolar solvent (S1, *n*-octane) and a polar solvent (S2, a dialkyl ether) varies with solvent composition as illustrated

in Figure 4b.<sup>30</sup> A linear relationship between  $\log K$  and  $\log [\text{polar solvent}]$  is observed as the concentration of the more polar solvent is decreased, until the value of  $\log K$  matches that obtained in pure alkane, after which there is no further change as a function of  $[\text{polar solvent}]$ . This is identical to the behavior observed in the adhesion force measurements. The relationship between the solution-phase association constant for formation of a 1:1 complex,  $K$ , and  $[\text{polar solvent}]$  shown in Figure 4b can be described by eq 1.

$$K = \frac{K_1}{1 + K_S[\text{polar solvent}]} \quad (1)$$

where  $K_1$  is the association constant for formation of a 1:1 complex between D and A in pure S1, and  $K_S$  is the equilibrium constant for solvation of D by S2 in solvent S1.

This result is a consequence of the fact that ethers and alkanes have hydrogen bond donor groups that have very similar properties, and so the only interaction of consequence that changes in solvent mixtures is solvation of D by the ether oxygens. Ether–alkane mixtures are very similar to the solvent mixtures investigated in the adhesion force measurements. Acetone and ethyl acetate have CH hydrogen bond donor groups, which are only slightly more polar than alkane CH groups, and so the only interaction that changes significantly in mixtures of alkanes and the more polar solvents is the solvation of the surface bound carboxylic acid hydrogen bond donor groups (D) by the solvent carbonyl oxygens (S2). The values of solution-phase equilibrium constants for formation of 1:1 complexes in pure solvents can be estimated using eq 2 in conjunction with Hunter's hydrogen bond parameters, which are related to the polarity of the functional groups involved in making pairwise intermolecular interactions:

$$-RT \ln K = -(\alpha - \alpha_S)(\beta - \beta_S) + 6 \text{ kJ mol}^{-1} \quad (2)$$

where  $\alpha$  is the hydrogen bond donor parameter for D,  $\beta$  is the hydrogen bond acceptor parameter for A,  $\alpha_S$  and  $\beta_S$  are the corresponding hydrogen bond donor and acceptor parameters for the solvent,<sup>31</sup> and the constant of  $6 \text{ kJ mol}^{-1}$  is the free energy penalty for formation of a bimolecular complex between two solutes.

Thus it is possible to use eq 2 to estimate the value of the solution-phase equilibrium constant for solvation of a carboxylic acid H-bond donor by acetone and by ethyl acetate in heptane. These equilibrium constants correspond to the values of  $K_S$  in Figure 4b and hence can be used to estimate the location of the intersection point of the two straight lines on the  $\log [\text{polar solvent}]$  axis in Figure 4a. Using the literature values for the hydrogen bond parameters in eq 2 gives  $K_S = 22 \text{ M}^{-1}$  for acetone and  $K_S = 15 \text{ M}^{-1}$  for ethyl acetate. These equilibrium constants correspond to intersection points at  $\log [\text{polar solvent}]$  of  $-1.3$  (corresponding to  $0.05 \text{ mol dm}^{-3}$ ) for acetone/heptane mixtures and  $-1.2$  (corresponding to  $0.07 \text{ mol dm}^{-3}$ ) for ethyl acetate/heptane mixtures. The degree of agreement between these calculated values and the experimental data in Figure 4a is striking and suggests that solvation thermodynamics of the surface bound functional groups does not differ significantly from solvation of individual molecules in solution. The effect of solvent on the surface adhesion forces can therefore be understood based on the thermodynamic properties of individual functional group interactions rather than bulk properties of the liquid or the surface.

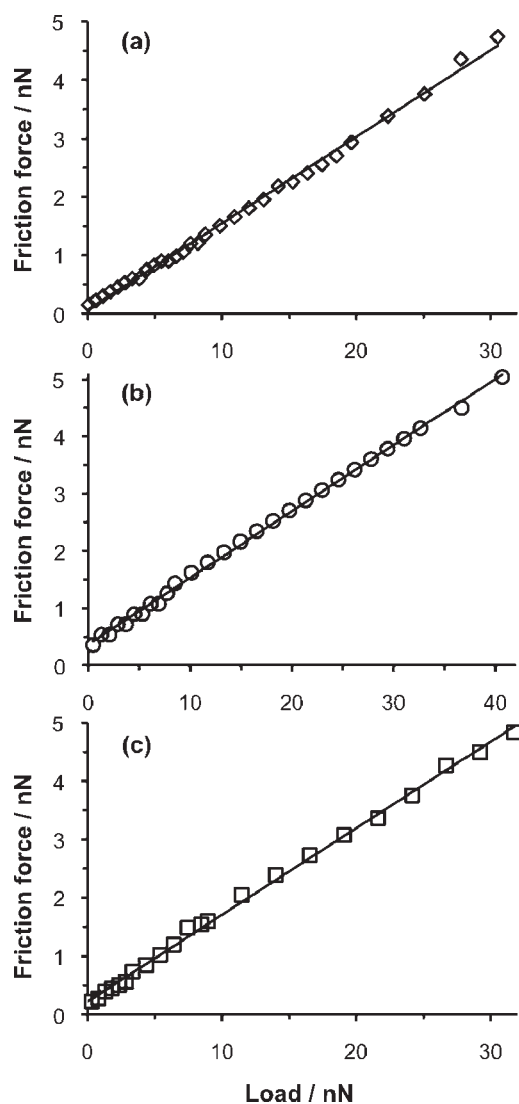


**Figure 5.** Friction–load plots in polar solvents. (a) Ethanol; (b) acetone; (c) ethyl acetate. The error bars are smaller than the size of the symbols used to mark points.

**Measurement of Friction Forces.** The friction force was measured as a function of the load in polar media (Figure 5). In ethanol, acetone, and ethyl acetate, the friction force was observed to increase in a linear fashion as the load was increased. A straight line was fitted to each plot using linear regression. It is significant to note that the line passes close to the origin in each case. Although the  $y$ -intercept is in each case slightly larger than the standard error in the friction force, we nevertheless believe that the magnitude of the intercept is within the bounds of expectation due to experimental error: in addition to random error, there is, additionally, the potential for systematic error arising from uncertainty in the photodetector signal corresponding to zero lateral force. While great care was exercised to eliminate such an error, a small uncertainty remains.

The observation of a linear friction–load relationship is consistent with Amontons’ law. Coefficients of friction were thus determined from the gradients of the friction–load plots. They were found to be 0.15, 0.12, and 0.15 for ethanol ( $\epsilon_r = 24.3$ ), acetone ( $\epsilon_r = 20$ ), and ethyl acetate ( $\epsilon_r = 6.0$ ) respectively, indicating that, in these polar media, the coefficient of

friction does not vary with the dielectric properties of the liquid medium.

Friction–load plots were acquired in liquid media containing decreasing amounts of the polar solvent. For mixtures containing largely the polar component, friction–load plots were linear (Figure 6). At approximately 1:1 mixtures of the two liquids, corresponding to a pull-off force of ca. 1 nN, a transition to nonlinear behavior was observed. The friction–load plots were analyzed using the General Transition Equation (GTE) developed by Carpick et al.<sup>32</sup> Analysis using the GTE yields a “transition parameter”,  $\alpha_{\text{GTE}}$ , that may be used to gauge whether DMT or JKR mechanics fits the behavior best. In general, values of  $\alpha_{\text{GTE}}$  close to zero were obtained, suggesting that the data fitted DMT mechanics, according to which model the area of contact  $A$  between the tip and surface (assumed, after Tabor,<sup>33</sup> to be proportional to the friction force) is:

$$A = \pi \left( \frac{R}{K} \right)^{2/3} (F_N + 4\pi\gamma R)^{2/3} \quad (3)$$

where  $R$  is the radius of the tip,  $K$  is the modulus, and  $\gamma$  is the surface free energy of the tip and substrate. Subsequent fitting using the DMT equation confirmed this.

Friction–load plots were also obtained in pure nonpolar liquids (Figure 7). In heptane, toluene, decane, dodecane, and hexadecane (pull-off forces ranging from 2.3 to 5.9 nN), the friction–load relationship was found to be consistent with the DMT model. However, in perfluorodecalin, which yielded a much larger pull-off force of 12.0 nN, the behavior was found to be consistent with the JKR model.

## DISCUSSION

**Adhesion forces for carboxylic acid terminated SAMs in liquid media may be interpreted in terms of the degree of solvation of the surface.** Our initial hypothesis was that changes in the dielectric properties of the liquid medium may influence the strength of interaction between the SFM tip and the sample. The data in Figures 2 and 3 demonstrate that while liquids with small dielectric constants do, in general, yield larger pull-off forces than liquids with large dielectric constants, liquids with the same dielectric constant may yield very different adhesion forces, and the same adhesion force may be obtained for liquids with a range of dielectric constants. The full explanation for the change in the pull-off force with liquid composition, and of the change in contact mechanics, thus lies elsewhere.

The correlation between the solvent-dependence of the experimental pull-off force data and the equilibrium constant for formation of a 1:1 H-bonded complex in solution is striking (Figure 4). This result implies that the pull-off force measurements can be understood on the basis of simple H-bond equilibria, where solvation and the thermodynamic properties of interactions involving surface-bound groups are the same as those for solution-phase equilibria. For liquid mixtures in which the surface-bound carboxylic acid groups are strongly solvated by the more polar solvent, the pull-off force measured for a SAM-coated sample and tip was small. As [polar solvent] decreased and the driving force for solvation of the carboxylic acid surface by the competitive polar solvent decreased, the magnitude of the pull-off force increased correspondingly. The adhesion force reached a limiting value at a polar solvent concentration equal to the solution-phase equilibrium constant for solvation of a

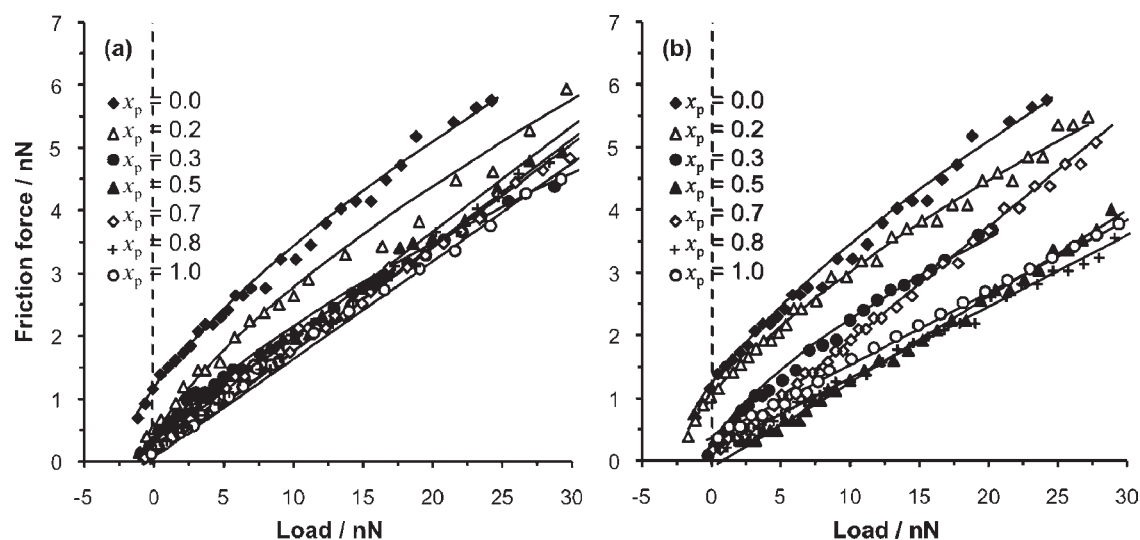


**Figure 6.** Friction–load plots in (a) ethyl acetate/heptane mixtures and (b) acetone/heptane mixtures of varying composition, where mole fraction  $x_p = 0$  corresponds to pure heptane. The error bars are smaller than the size of the symbols used to mark points.

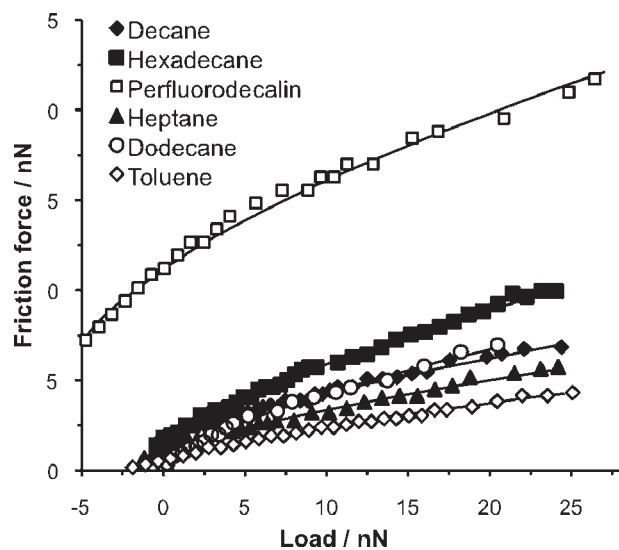


**Figure 7.** Friction–load relationships in nonpolar liquids. The error bars are smaller than the size of the symbols used to mark points.

carboxylic acid by a dilute solution of the polar component in the nonpolar solvent,  $K_S$ . The pull-off force measured at this point equals the strength of interaction between surface-bound carboxylic acid groups in a nonpolar medium.

That the variation in the pull-off force with solvent composition correlates so closely with the thermodynamics of solution-phase association between carboxylic acid groups and polar solvent molecules is surprising. According to standard treatments of adhesion, the work of adhesion between the tip (T) and the sample (S) is determined by the equilibrium at the tip–sample contact. Three phase boundaries exist (tip–sample, tip–liquid, and sample–liquid), so the tip–sample work of adhesion in the presence of a liquid (L) is equal to

$$W_{\text{TLS}} = \gamma_{\text{TL}} + \gamma_{\text{SL}} - \gamma_{\text{TS}} \quad (4)$$

where  $\gamma_{\text{TL}}$  is the tip–liquid interfacial free energy,  $\gamma_{\text{SL}}$  is the sample–liquid interfacial free energy, and  $\gamma_{\text{TS}}$  is the tip–sample

interfacial free energy.<sup>34</sup> The tip–solvent and sample–solvent interfacial free energies will be strongly influenced by the thermodynamics of association between solvent molecules and adsorbates. However, that there is apparently such a precise correlation between the solution-phase carboxylic acid–polar solvent association constant and the thermodynamics of tip–sample adhesion is unexpected, the more so because the pull-off experiment is expected to be a nonequilibrium process.

There have been few studies of pull-off forces in liquid mixtures. However, Vezenov et al. measured pull-off forces for carboxylic acid terminated SAMs in methanol–water mixtures.<sup>35</sup> A significant difference between their study and ours is that both methanol and water are expected to solvate carboxylic acid functionalized surfaces, because both liquids possess the capacity to form hydrogen bonds. Moreover, their data were not analyzed in terms of the solution-phase association behavior. Nevertheless, they postulated that, for liquid media that could form hydrogen-bonding interactions with the tip and sample surface, solvation effects influence the strength of the adhesion force.

Our data support the suggestion that solvation effects influence the adhesion force but go further. In particular, Figure 4a suggests that pull-off force data enable the equilibrium constant for solvation of the carboxylic acid surface by the polar solvent to be determined, simply by fitting a line to a plot of the pull-off force against [polar solvent] and determining the concentration at which the pull-off force intercepts that measured in the pure nonpolar solvent. Analysis of pull-off forces thus provides a means to explore surface solvation phenomena in a quantitative fashion. The possibility of using pull-off force data in this way has not been explored previously, but it seems to be a powerful predictive capability.

**Contact mechanics are correlated with the strength of adhesion between the tip and the surface.** For liquids in which small adhesion forces were measured, a linear friction–load relationship was obtained. As [polar solvent] was decreased, and the pull-off force increased above ca. 1 nN, the friction–load behavior began to change, and for liquids yielding pull-off forces larger than 1.5 nN and smaller than 6 nN, the behavior was found to fit DMT mechanics. Only in perfluorodecalin (adhesion force

of 12 nN) was JKR-type behavior observed. These data strongly suggest that linear friction–load relationships (ie ones that are described by Amontons' law) are associated with systems with weak adhesion between the tip and the sample. For surfaces in which there is modest or strong adhesion, single asperity contact mechanics models appear to describe the experimental data better. On a practical note, we observed that where there was a linear friction–load relationship, a line fitted through the points by linear regression passed through the origin, or at least very close to it. Where a substantial nonzero intercept with the vertical axis was observed, the mechanics was found to obey a single asperity mechanics model.

For SAMs<sup>36</sup> and for poly(ethylene terephthalate) films<sup>19</sup> it was previously reported that, in perfluorodecalin, large adhesion forces were measured and the friction–load data were found to be consistent with JKR mechanics, while, in ethanol, adhesion forces were small and Amontons' law was found to fit the data. Our original explanation was that the small dielectric constant of perfluorodecalin, compared to ethanol, caused an increase in the Hamaker constant, leading to stronger adhesion. The data in Figure 2 suggest that this is not a complete explanation. However, the conclusion that strong adhesion yields single asperity contact mechanics is supported by the present data.

In the present study, small adhesion forces were measured for liquid mixtures which were expected to yield high degrees of solvation of the surface carboxylic acid groups. Hence in these hydrogen-bonding systems, a high degree of surface solvation was correlated with behavior consistent with Amontons' law. A linear friction–load relationship was, moreover, only observed for highly solvated surfaces. The transition from Amontons-type to DMT-type behavior occurs at a pull-off force of ca. 1 nN, where the surface is extensively solvated by the polar solvent: at this point, [polar solvent] is an order of magnitude larger than  $1/K_S$  (see Figure 4a), so the carboxylic acid H-bond donor groups are 90% solvated by the polar solvent. When the surface is less strongly solvated, DMT-type behavior is observed. Thus DMT-type behavior appears, for the systems studied here, to be normal, and Amontons' law describes a limiting situation where there is unusually low adhesion between the tip and surface. We hypothesize that extensive solvation reduces the barrier to surface shear, in the same way that it reduces the work of adhesion perpendicular to the surface plane, minimizing the amount of energy dissipated in shearing. Consequently friction arises purely from the shearing of dispersion interactions and from energy dissipation in the deformation of molecular structure through the creation of gauche defects and other pathways.<sup>37–41</sup>

**The friction force is best understood to be the sum of load-dependent and shear terms.** A priori, it might be expected that a scanning force microscope probe, representing an idealized asperity, would yield single asperity contact mechanics. The observation of a linear friction–load relationship by many authors appeared for a long time to be surprising. One explanation for such reports was that over a restricted range of load, especially under only compressive loading, a system that obeyed DMT or JKR mechanics may appear to yield a linear friction–load relationship. An alternative explanation was that plastic deformation, or multiple asperity contacts with the surface, may cause pseudomacroscopic behavior. However, the observation of single asperity mechanics under strongly adhesive conditions both in the present work and in previous studies refutes these explanations. The work of Gao et al. suggests an alternate explanation: that linear friction–load relationships are

normative, and single asperity behavior represents a limiting case. In our earlier work,<sup>19,36</sup> this seemed to be an attractive explanation. However, examination of a broad range of liquid mixtures of varying compositions in the present study has provided a much more comprehensive picture of the influence of the fluid medium. Single asperity mechanics appear to be normative; they apply for the majority of the liquid mixtures studied here and for all liquids where the surface was not strongly solvated. Thus a linear friction–load relationship is a limiting case representing a fully solvated surface for which the only adhesive interactions are weak dispersion forces.

Given the range of behavior observed in the present study, the most natural explanation is that the friction force is the sum of two terms, a load-dependent term and a shear term, as has been proposed by others:<sup>4</sup>

$$F_F = \mu F_N + \sigma A \quad (5)$$

where  $\sigma$  is the surface shear strength and  $A$  is the area of contact. In pure acetone and ethyl acetate, the shear term  $\sigma A$  is negligible and a linear friction–load relationship is observed. As [polar solvent] decreases, the shear term increases in magnitude until the mole fraction of heptane is 0.7, after which the behavior is so dominated by the shear term that it is in close conformity with the DMT model. For the SAM systems studied here, we may further expand eq 5, using the area of contact in the DMT model:

$$F_F = \mu F_N + \sigma \left( \frac{R}{K} \right)^{2/3} [F_N + F_{adh}]^{2/3} \quad (6)$$

While Gao et al. emphasized the area of contact is not a fundamental quantity,<sup>18</sup> it is nevertheless the case in DMT theory that the force of adhesion  $F_{adh} = 2\pi WR$ , where  $W$  is the work of adhesion, and thus it is axiomatic that, for a well-defined material, the interaction force scales with both the area of contact and the number of interacting molecular pairs. Consequently, bearing in mind the close correlation between the solvent-dependence of the pull-off data in Figure 4a and the solution-phase equilibrium constants in Figure 4b, we conclude that molecular level interaction energies at surfaces may be determined from analysis of the contact mechanics using DMT theory and compared with molar interaction free energies determined in studies of solution-phase association behavior. This provides a powerful new approach to the study of intermolecular interactions.

Finally, the significance of the observation of linear friction–load behavior needs to be established in more detail and should be the focus for future studies. For a fully solvated SAM surface, only dispersion forces act across the sliding contact and these are plainly weak enough for the shear term in eq 5 to be negligible. Presumably, the load-dependent modes of energy dissipation that operate are simply mechanical deformations of the alkyl chains in both the bound solvent molecules and also the underlying adsorbate molecules.<sup>37–41</sup> This may be likened to a molecular-scale plowing effect,<sup>42</sup> albeit with a small net deformation given the finite depth of the molecular layer and the small loads (explaining the small coefficients of friction reported here). Undoubtedly, the contribution of the load-dependent term may be greater in materials that provide more pathways for deformation-induced energy dissipation, such as monolayers of alkylsilanes,<sup>42</sup> which are less well ordered than alkylthiolate SAMs, and polymer brushes,<sup>43–45</sup> for which many modes of chain deformation are accessible. Hence the relative magnitudes



of the pressure-dependent and shear terms are likely to vary depending on the material structure.

## CONCLUSIONS

Adhesion forces between carboxylic acid terminated SAMs measured using a scanning force microscope are in striking agreement with predictions of solution-phase equilibrium constants made using a simple model, in which the solvation thermodynamics of the carboxylic acid groups may be predicted by considering the concentration and polarity of the functional groups in the liquid. In particular, the solvent-dependence of the 1:1 association constant for formation of a H-bonded complex in solution,  $\log K$ , is identical to the behavior of  $F_{\text{adh}}$  measured in the pull-off experiment, and the equilibrium constant describing solvation of the carboxylic acid by the polar solvent,  $K_S$ , which can be estimated using both approaches is found to be in good agreement. When  $[\text{polar solvent}] < 1/K_S$ , the adhesion force is invariant with concentration, while, for higher values of  $[\text{polar solvent}]$ , the adhesion force decreases monotonically with increasing values of  $[\text{polar solvent}]$  as the SAM surface becomes increasingly highly solvated. While adhesion forces are larger in media with small dielectric constants than in media with large dielectric constants, the correlation between adhesion and dielectric constant is nevertheless weak. Friction forces measured using friction force microscopy correlate with variations in the solvation thermodynamics of the SAM surface, with the mechanics changing from a single asperity type of behavior (a nonlinear friction–load relationship) to one consistent with Amontons' law (a linear friction–load relationship) as the surface becomes fully solvated. The friction–load relationships can be rationalized if the friction force is treated as the sum of load-dependent and shear terms. In pure acetone and ethyl acetate, the SAM surface is fully solvated and the shear term is negligible. The load-dependent term dominates, and a linear friction–load relationship is observed. For liquid mixtures, as  $[\text{polar solvent}]$  decreases, the degree of surface solvation decreases and the shear term dominates the friction force. A nonlinear friction–load relationship is observed in liquid media that yield pull-off forces between 1.5 and 6 nN, and the data are consistent with DMT mechanics. In perfluorodecalin, a very large adhesion force is observed, and the data are consistent with JKR mechanics.

## AUTHOR INFORMATION

### Corresponding Author

graham.leggett@sheffield.ac.uk

## ACKNOWLEDGMENT

The Authors thank the Engineering and Physical Sciences Research Council (Grant EP/039999/1) for financial support.

## REFERENCES

- (1) Bowden, F. P.; Tabor, D. *The Friction and Lubrication of Solids*; Oxford University Press: Oxford, 1950.
- (2) Mate, C. M. *Tribology on the small scale*; Oxford University Press: Oxford, 2008.
- (3) Overney, R.; Meyer, E. *MRS Bull.* **1993**, 26.
- (4) Carpick, R. W.; Salmeron, M. *Chem. Rev.* **1997**, 97, 1163.
- (5) Gnecco, E.; Bennewitz, R.; Gyalog, T.; Meyer, E. *J. Phys.: Condens. Matter* **2001**, 13, R619.
- (6) Vezenov, D. V.; Noy, A.; Rozsnyai, L. F.; Lieber, C. M. *J. Am. Chem. Soc.* **1997**, 119, 2006.

- (7) Frisbie, C. D.; Rozsnyai, L. F.; Noy, A.; Wrighton, M. S.; Lieber, C. M. *Science* **1995**, 265, 2071.
- (8) McDermott, M. T.; Green, J.-B. D.; Porter, M. D. *Langmuir* **1997**, 13, 2504.
- (9) Beake, B. D.; Leggett, G. J. *Langmuir* **2000**, 16, 735.
- (10) Brewer, N. J.; Beake, B. D.; Leggett, G. J. *Langmuir* **2001**, 16, 735.
- (11) Kim, H. I.; Houston, J. E. *J. Am. Chem. Soc.* **2000**, 122, 12045.
- (12) Clear, S. C.; Nealey, P. F. *Langmuir* **2001**, 17, 720.
- (13) Kim, H. I.; Koini, T.; Lee, T. R.; Perry, S. S. *Langmuir* **1997**, 13, 7192.
- (14) Brewer, N. J.; Foster, T. T.; Leggett, G. J.; Alexander, M. R.; McAlpine, E. O. *J. Phys. Chem. B* **2004**, 108, 4723.
- (15) Piner, R. D.; Zhu, J.; Xu, F.; Hong, S.; Mirkin, C. A. *Science* **1999**, 283, 661.
- (16) Chong, K. S. L.; Sun, S.; Leggett, G. J. *Langmuir* **2005**, 21, 3903.
- (17) Whittle, T. J.; Leggett, G. J. *Langmuir* **2009**, 25, 2217.
- (18) Gao, J.; Luedtke, W. D.; Gourdon, D.; Ruths, M.; Israelachvili, J. N.; Landman, U. *J. Phys. Chem. B* **2004**, 108, 3410.
- (19) Hurley, C. R.; Leggett, G. J. *Langmuir* **2006**, 22, 4179.
- (20) Whittle, T. J.; Leggett, G. J. *Langmuir* **2009**, 25, 9182.
- (21) Ruths, M. *J. Phys. Chem.* **2006**, 110, 2209.
- (22) Mo, Y.; Turner, K. T.; Szlufarska, I. *Nature* **2009**, 457, 1116.
- (23) Lo, Y.-S.; Huefner, N. D.; Chan, W. S.; Dryden, P.; Hagenhoff, B.; Beebe, T. P. *Langmuir* **1999**, 15, 6522.
- (24) Hutter, J. L.; Bechhoeffer, J. *Rev. Sci. Instrum.* **1993**, 64, 1868.
- (25) Varenberg, M.; Etsion, I.; Halperin, G. *Rev. Sci. Instrum.* **2003**, 74, 3362.
- (26) Tocha, E.; Schonherr, H.; Vancso, G. J. *Langmuir* **2006**, 22, 2340.
- (27) Grierson, D. S.; Flater, E. E.; Carpick, R. W. *J. Adhesion Sci. Technol.* **2005**, 19, 291.
- (28) <http://nanoprobenetwork.org/welcome-to-the-carpick-labs-software-toolbox>.
- (29) Kerchove, F. v. d.; Vijlder, M. D. *J. Chem. Eng. Data* **1977**, 22, 333.
- (30) Buurma, N. J.; Cook, J. L.; Hunter, C. A.; Low, C. M. R.; Vinter, J. G. *Chem. Sci.* **2010**, 1, 242.
- (31) Hunter, C. A. *Angew. Chem., Int. Ed.* **2004**, 43, 5310.
- (32) Carpick, R. W.; Ogletree, D. F.; Salmeron, M. *J. Colloid Interface Sci.* **1999**, 211, 395.
- (33) Bowden, F. P.; Tabor, D. *The Friction and Lubrication of Solids*; Oxford University Press: Oxford, 1950 (reprinted 2001).
- (34) Israelachvili, J. N. *Intermolecular and Surface Forces*, 2nd ed.; Academic Press: London, 1992.
- (35) Vezenov, D. V.; Zhuk, A. V.; Whitesides, G. M.; Lieber, C. M. *J. Am. Chem. Soc.* **2002**, 124, 10578.
- (36) Colburn, T. J.; Leggett, G. J. *Langmuir* **2007**, 23, 4959.
- (37) Tutein, A. B.; Stuart, S. J.; Harrison, J. A. *J. Phys. Chem. B* **1999**, 103, 11357.
- (38) Mikulski, P. T.; Harrison, J. A. *Tribol. Lett.* **2001**, 10, 29.
- (39) Mikulski, P. T.; Harrison, J. A. *J. Am. Chem. Soc.* **2001**, 123, 6873.
- (40) Mikulski, P. T.; Herman, L. A.; Harrison, J. A. *Langmuir* **2005**, 21, 12197.
- (41) Mikulski, P. T.; Gao, G.; Chateaufneuf, G. M.; Harrison, J. A. *J. Chem. Phys.* **2005**, 122, 024701.
- (42) Flater, E. E.; Ashurst, W. R.; Carpick, R. W. *Langmuir* **2007**, 23, 9242.
- (43) Müller, M.; Lee, S.; Spikes, H. A.; Spencer, N. D. *Tribol. Lett.* **2003**, 15, 395.
- (44) Muller, M. T.; Yan, X.; Lee, S.; Perry, S. S.; Spencer, N. D. *Macromolecules* **2005**, 38, 5706.
- (45) Limpoco, F. T.; Advincula, R. C.; Perry, S. S. *Langmuir* **2007**, 23, 12196.